

## Controlling the cavity field with enhanced Kerr nonlinearity in three-level atoms

Hai Wang,\* David Goorskey, and Min Xiao

*Department of Physics, University of Arkansas, Fayetteville, Arkansas 72701*

(Received 15 January 2002; published 2 May 2002)

We experimentally demonstrate cavity field control by another laser beam with three-level  $\Lambda$ -type atoms inside an optical ring cavity. By adjusting the frequency detuning of the controlling beam (coupled to one of the atomic transitions), the intensity of the cavity field interacting with another atomic transition is switched on and off. Such all-optical switching between two steady states is caused by the enhanced Kerr nonlinearity due to atomic coherence in such system.

DOI: 10.1103/PhysRevA.65.051802

PACS number(s): 42.50.Gy, 42.65.-k, 32.80.Qk

The essential element in all-optical communication and optical computation is to achieve effective and fast all-optical switching. Multilevel electromagnetically induced-transparency (EIT) systems are ideal for such applications, since the linear and nonlinear optical properties of the probe beam can be dramatically changed by another (controlling) laser beam due to atomic coherence [1–11]. When such an EIT medium is placed inside an optical cavity, many other interesting effects, such as cavity linewidth narrowing [12], optical bistability [13,14], and dynamic instability [13], appear. The Kerr-nonlinear index of refraction of a three-level  $\Lambda$ -type atomic system can be greatly enhanced near resonance (by two orders of magnitude in some frequency detuning regions) and can change sign with small changes (tens of megahertz) in the frequency detunings of the controlling beam or cavity (probe) field [15]. Such enhancement in Kerr nonlinearity is caused by the atomic coherence induced in this EIT medium.

With the knowledge of these dramatic changes of the Kerr-nonlinear index of refraction near resonance, we demonstrate that the cavity-field intensity can be controlled by the frequency detuning of the controlling field at a relatively low optical power. With a small frequency change of the controlling beam (24 MHz), the cavity-field intensity switches with a switching ratio better than 30:1 and a switching time of few microseconds. Such all-optical switching is fundamentally interesting and can have applications in all-optical communication, optical logic gates, and optical information processing.

The experiment is performed in a composite system consisting of a collection of three-level  $\Lambda$ -type rubidium atoms, as shown in Fig. 1, in an atomic vapor cell and an optical ring cavity.  $F=1$  (state  $|1\rangle$ ) and  $F=2$  (state  $|3\rangle$ ) states of  $5S_{1/2}$  are the two lower states and  $F'=2$  state (state  $|2\rangle$ ) of  $5P_{1/2}$  serves as the upper state. The controlling (coupling) laser beam (with frequency  $\omega_c$ ) couples states  $|3\rangle$  and  $|2\rangle$  while the switching (probe) beam (with frequency  $\omega_p$ ) interacts with states  $|1\rangle$  and  $|2\rangle$ . The frequency detuning of the controlling beam is defined as  $\Delta_c = \omega_c - \omega_{23}$ , where  $\omega_{23}$  is the atomic frequency of the  $|3\rangle$  to  $|2\rangle$  transition, and the fre-

quency detuning of the switching beam from its atomic transition is defined as  $\Delta_p = \omega_p - \omega_{12}$ . As we have previously demonstrated, the Kerr-nonlinear index of refraction  $n_2$  changes dramatically both in magnitude and in sign near resonance [15]. These changes can be used to control the steady-state behaviors of the system. By changing the frequency detuning of the controlling beam, we can control the nonlinearity of the system and, therefore, make the output intensity of the cavity field to be at different steady states. Such action constitutes a controllable all-optical switching in this composite atom-cavity system.

A simplified sketch of the experimental setup is shown in Fig. 2 with an atomic vapor cell containing three-level atoms placed inside a three-mirror optical ring cavity. Both the controlling (LD1) and the switching (LD2) lasers are single-mode diode lasers that are current and temperature stabilized. The frequencies of these two diode lasers are further stabilized by using optical feedback through servo-loop-controlled mirrors. Parts (about 10%) of the switching and controlling beams are split by polarizing beam splitters PB2 and PB4 to a saturation absorption spectroscopy setup for monitoring the frequency detunings of the two lasers from their respective resonances with atomic transitions. The flat mirror  $M2$  and the concave mirror  $M1$  ( $R=10$  cm) have about 1% and 3% intensity transmissions, respectively. The third cavity mirror (concave with  $R=10$  cm) is mounted on a piezoelectric transducer (PZT) with reflectivity larger than 99.5%. The finesse of the empty cavity is about 100 with a free spectral range of 822 MHz (cavity length is 37 cm). A third laser (reference beam) is used to lock the frequency of the optical cavity to a Fabry-Perot cavity, which can be tuned easily by a PZT mounted on one of the mirrors. The ru-

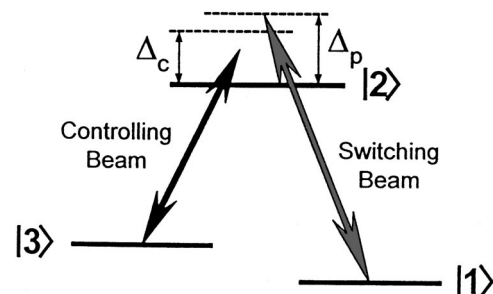


FIG. 1. Sketch of a three-level  $\Lambda$ -type atomic system.

\*Present address: Institute of Opto-Electronics, Shanxi University, Shanxi, Taiyuan, China.

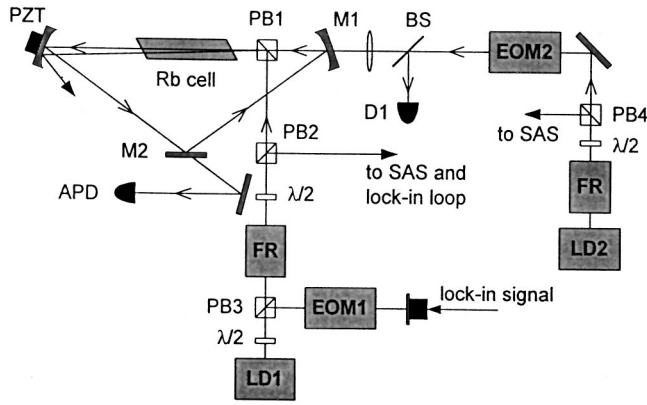


FIG. 2. Experimental setup. SAS: a saturation atomic spectroscopy setup for frequency references of the laser beams. EOM1: electro-optical modulator for phase control of the controlling beam. EOM2: scanning the cavity input power of the switching beam. FRs: Faraday rotators. PZT is for scanning the cavity length.

bidium vapor cell is 5 cm long with Brewster windows and is wrapped in  $\mu$  metal for magnetic shielding and heated to 72 °C. The switching field enters the cavity through mirror  $M1$  and circulates inside the optical ring cavity. The controlling beam is introduced through the polarization beam splitter  $PB1$  with an orthogonal polarization to the cavity field and is misaligned by a small angle ( $<1^\circ$ ) to avoid its circulation inside the optical cavity. The radii of the controlling and switching beams at the center of the atomic cell are estimated to be 700 and 80  $\mu\text{m}$ , respectively. With the reflection losses from the  $PB1$  and the windows of the atomic cell, the cavity finesse (with rubidium atoms far off resonance) is degraded to about 50. The cavity input intensity of the switching field is controlled by an electro-optical modulator (EOM2). The frequency detunings of the two beams are measured by a Fabry-Perot cavity in reference to the atomic saturation spectrum. One of the important advantages of the current experimental setup shown in Fig. 2 is the use of a two-photon Doppler-free configuration by propagating the controlling beam colinearly with the cavity field inside the atomic cell, which eliminates the first-order Doppler effect for the cavity field [4].

In this experiment, we first measure the absorption spectrum of the switching field by scanning  $\Delta_p$  for fixed controlling power ( $P_c = 14.3$  mW) and cavity input power ( $P_p^{\text{in}} = 390$   $\mu\text{W}$ ). The switching frequency  $\Delta_c$  is chosen to jump back and forth between 111 and 135 MHz, where the absorption is small and same for these two frequencies. The frequency switching of the controlling beam (between  $\Delta_c = 111$  and 135 MHz) is achieved by phase modulating the controlling beam in the path of the optical feedback with another electro-optical modulator (EOM1). The modulation frequency for a square-wave signal on the EOM1 is 58 kHz with a rising time  $<1$   $\mu\text{s}$ . Then, we stop the frequency scan of  $\Delta_p$  and lock it to  $\Delta_p = 123$  MHz (which is midway between the two alternating frequencies of the controlling beam and serves as the operation point). The ring cavity length is scanned (with a rate of 0.903  $\mu\text{m}/\text{ms}$ ) from longer to shorter by a ramp voltage on the PZT for  $\Delta_c = 135$  ( $\Delta_p$

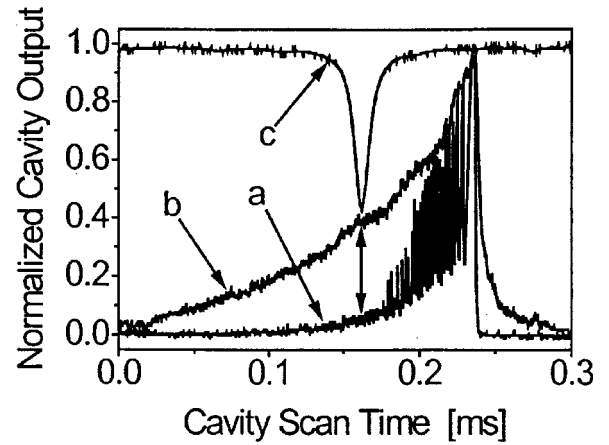


FIG. 3. Cavity transmission via cavity length scan. Curve  $a$  is for  $\Delta_c = \Delta_p - 12$  MHz with  $\Delta_p = 123$  MHz,  $P_p^{\text{in}} = 0.39$  mW, and  $P_c = 14.3$  mW; curve  $b$  is for  $\Delta_c = \Delta_p + 12$  MHz with other parameters the same; curve  $c$  is the frequency of the reference laser beam used to lock the ring cavity.

+12 MHz) and  $\Delta_c = 111$  MHz ( $\Delta_p - 12$  MHz), respectively. The cavity transmission profiles are shown in Fig. 3. As one can see that for  $\Delta_c = 111$  MHz (curve  $a$ ), the cavity transmission profile is narrower, which gives a smaller Kerr-nonlinear index of refraction ( $n_2 = -0.8 \times 10^{-7}$   $\text{cm}^2/\text{W}$ ) [15]. The oscillation on the left side of the transmission peak is due to optical instability in this system and has been studied in detail in Ref. [13]. However, for  $\Delta_c = 135$  MHz (curve  $b$ ), the cavity transmission profile becomes highly asymmetric corresponding to a much larger Kerr-nonlinear index of refraction ( $n_2 = 6 \times 10^{-7}$   $\text{cm}^2/\text{W}$ ), which is determined by the degree of asymmetry of this cavity transmission profile due to the nonlinear phase shift [15]. Curve  $c$  shows the (inverted) cavity output of a frequency-locked reference beam detuned far from atomic resonances as the cavity length is scanned.

After choosing the optimal operation position for the optical cavity detuning (indicated by the arrow) from Fig. 3, the optical ring cavity is frequency locked onto the cavity transmission peak of this reference laser beam, which counter-propagates with the first two laser beams. The cavity detuning ( $\Delta_\theta$ ) is defined by the frequency difference between resonance of the reference beam (peak of curve  $c$ ) and the peak of curve  $b$  in Fig. 3. With the optical cavity locked to a cavity detuning of  $\Delta_\theta = 65$  MHz, we then scan the input cavity power for the same two frequency detunings of the controlling beam. The frequency detuning ( $\Delta_p$ ) of the cavity field is set at the middle of the two  $\Delta_c$  values, i.e.,  $\Delta_p = 123$  MHz, as shown in Figs. 4(a) and 4(b), respectively. Optical bistability clearly appears in Fig. 4(b) with a quite low threshold power (0.3 mW) when the nonlinear index  $n_2$  is larger ( $n_2 \approx 6 \times 10^{-7}$   $\text{cm}^2/\text{W}$ ) for  $\Delta_c = 135$  MHz. When the nonlinear index is lower and has a negative sign ( $n_2 \approx -0.8 \times 10^{-7}$   $\text{cm}^2/\text{W}$ ) for  $\Delta_c = 111$  MHz, the threshold increases dramatically and bistability appears at a much higher input power beyond the input power range (0.6 mW) shown in Fig. 4(a). The large intensity range of the cavity field at the upper branch of the bistable curve of Fig. 4(b) is due to

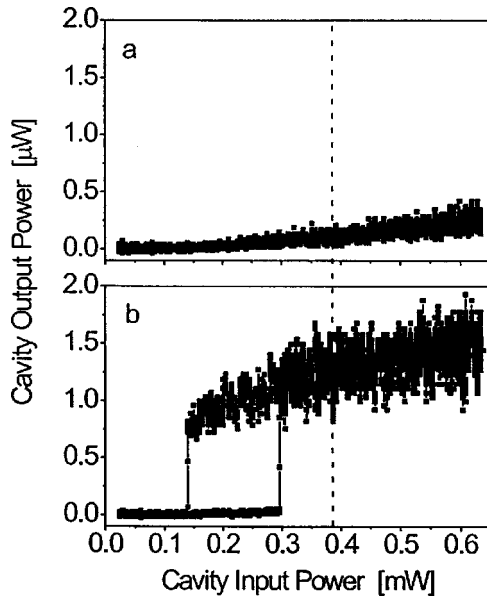


FIG. 4. Cavity transmission power vs cavity input power. These are the steady-state curves of the system for (a)  $n_2 = -0.8 \times 10^{-7} \text{ cm}^2/\text{W}$  ( $\Delta_c = \Delta_p - 12 \text{ MHz}$ ) and (b)  $n_2 = 6 \times 10^{-7} \text{ cm}^2/\text{W}$  ( $\Delta_c = \Delta_p + 12 \text{ MHz}$ ), respectively. The cavity input power of the switching beam is set at 0.39 mW with all other parameters the same as in Fig. 3.

the combined effects of stability of the optical cavity (whose input intensity scans up and, then, down to observe this bistable curve) and an oscillation behavior (possibly dynamic instability, as observed in the case of two-level atoms inside an optical cavity [16]), which is currently under investigation. Finally, we set the cavity input power to be  $P_p^{\text{in}} = 0.39 \text{ mW}$ . When the controlling frequency detuning is switched between  $\Delta_c = \Delta_p + 12$  and  $\Delta_c = \Delta_p - 12 \text{ MHz}$ , as shown in Fig. 5(b), the cavity output intensity is switched between two distinct steady-state values, as shown in Fig. 5(a). The average cavity output peak power of the “on” state is about  $1.2 \mu\text{W}$  and the average power of the “off” state is less than  $0.034 \mu\text{W}$ , which give a switching ratio of better than 30:1.

The mechanism of this switching phenomenon can be easily understood from Figs. 3 and 4. The two cavity transmission curves (*a* and *b*) in Fig. 3 correspond to two  $\Delta_c$  values for switching. When the optical cavity is frequency locked at  $\Delta_\theta = 65 \text{ MHz}$  (resonant position of curve *c*) and  $\Delta_c$  switches between the two values, the cavity transmission intensity also switches between the two steady-state values (curve *a* and curve *b* at the resonant position of curve *c*, as shown by the arrow in Fig. 3). For the given experimental parameters (such as  $\Delta_p$ ,  $I_c$ ,  $P_p^{\text{in}}$ , and  $\Delta_c$  values), the cavity detuning of  $\Delta_\theta = 65 \text{ MHz}$  gives the maximum switching ratio of better than 30:1. If the cavity is tuned closer to its resonance ( $\Delta_\theta < 65 \text{ MHz}$ ), the system becomes unstable. Looking at Fig. 4, one can see that the change of  $\Delta_c$  changes the steady-state curve of the system and forces the cavity field to operate at different intracavity intensities. One can also consider this switching action as a frequency-to-amplitude signal conversion since by modulating the frequency of one laser beam,

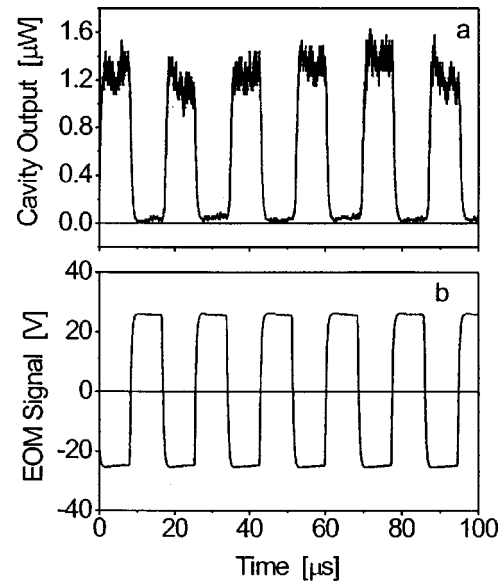


FIG. 5. Optical switching of the cavity field controlled by the controlling beam. (a) “On” and “off” states of the cavity field controlled by the voltage applied on EOM1, shown on (b), for two frequency detunings of  $\Delta_c = 111 \text{ MHz}$  (upper voltage level) and  $\Delta_c = 135 \text{ MHz}$  (lower voltage level), respectively.

the intensity of another laser beam is controlled. Such frequency-to-amplitude conversion could have significant applications in optical communication and optical information processing.

This all-optical switching is quite efficient since it only needs to switch the frequency detuning of the controlling beam by a small amount (24 MHz in this case) which, in turn, gives a switching ratio of better than 30:1 for the cavity output beam intensity. The switching speed of few  $\mu\text{s}$  in this work is currently only limited by the phase modulation frequency of our setup (the frequency of the driver for EOM1 is limited to 200 kHz for a sinusoidal wave form). Switching cavity transmission intensity with an even smaller change of the frequency detuning of the controlling beam should also be possible since, as demonstrated in our measurements of the Kerr-nonlinear index of refraction earlier [15], a 7-MHz change in  $\Delta_c$  can make  $n_2$  change from a maximum value of  $7 \times 10^{-6} \text{ cm}^2/\text{W}$  to zero at near resonance with a lower cavity input intensity of about  $10 \mu\text{W}$ . However, such an experimental demonstration requires better frequency stability of the lasers and the optical cavity. The choices of our frequency detunings ( $\Delta_p$  and  $\Delta_c$ ) of the two laser beams in the current experiment were for the stability and repeatability of the observed phenomena.

In summary, we have experimentally demonstrated an all-optical switch of the cavity transmission intensity by controlling the frequency detuning of another controlling beam in a three-level  $\Lambda$ -type atomic system inside an optical ring cavity. The dramatic change in the two steady states for different frequency detunings of the controlling beam is created by the large difference in the Kerr-nonlinear index of refraction enhanced by atomic coherence in such a three-level EIT system. This system provides a great advantage over the two-level atomic system since it has large enhanced nonlinearity

and offers control over the steady states of the system. Although the switching action is not between the two steady states of a single bistable curve, the current system is much more efficient and robust. The switching ratio can easily reach the level of 30:1 and a switching speed of microsecond. With further system optimization and technical improvements, we can improve the performance (in switching ratio and speed) of such all-optical switching, especially to

operate it at much lower (even at single-photon) intensity levels [17,18]. This kind of Kerr-nonlinearity-induced all-optical switching can find applications in optical communication, all-optical computation, and quantum information processing.

We acknowledge the funding support from the National Science Foundation.

- 
- [1] E. Arimondo, in *Progress in Optics*, edited by E. Wolf (North-Holland, Amsterdam, 1996), Vol. 35, p. 259.
- [2] S. E. Harris, *Phys. Today* **50**(7), 36 (1997).
- [3] K. J. Boller, A. Imamoglu, and S. E. Harris, *Phys. Rev. Lett.* **66**, 2593 (1991).
- [4] J. Gea-Banacloche, Y. Li, S. Jin, and M. Xiao, *Phys. Rev. A* **51**, 576 (1995); Y. Li and M. Xiao, *ibid.* **51**, R2703 (1995).
- [5] M. Xiao, Y. Li, S. Jin, and J. Gea-Banacloche, *Phys. Rev. Lett.* **74**, 666 (1995).
- [6] A. S. Zibrov *et al.*, *Phys. Rev. Lett.* **76**, 3935 (1996).
- [7] G. Z. Zhang, K. Hakuta, and B. P. Stoicheff, *Phys. Rev. Lett.* **71**, 3099 (1993).
- [8] P. Hemmer *et al.*, *Opt. Lett.* **21**, 1936 (1996).
- [9] B. Lu, W. H. Burkett, and M. Xiao, *Opt. Lett.* **23**, 804 (1998).
- [10] M. Jain *et al.*, *Phys. Rev. Lett.* **77**, 4326 (1996).
- [11] M. Yan, E. G. Rickey, and Y. Zhu, *Phys. Rev. A* **64**, R041801 (2001).
- [12] H. Wang, D. J. Goorskey, W. H. Burkett, and M. Xiao, *Opt. Lett.* **25**, 1732 (2000).
- [13] H. Wang, D. J. Goorskey, and M. Xiao, *Phys. Rev. A* **65**, R011801 (2002).
- [14] W. Harshawardhan and G. S. Agarwal, *Phys. Rev. A* **53**, 1812 (1996).
- [15] H. Wang, D. J. Goorskey, and M. Xiao, *Phys. Rev. Lett.* **87**, 073601 (2001).
- [16] L. A. Orozco, A. T. Rosenberger, and H. J. Kimble, *Phys. Rev. Lett.* **53**, 2547 (1984).
- [17] S. E. Harris and L. V. Hau, *Phys. Rev. Lett.* **82**, 4611 (1999); S. E. Harris and Y. Yamamoto, *ibid.* **81**, 3611 (1998).
- [18] A. Imamoglu, H. Schmidt, G. Woods, and M. Deutsch, *Phys. Rev. Lett.* **79**, 1467 (1997).